Near-surface seismic and EM imaging

Jide Ogunbo

Postdoctoral fellow,
Department of Earth, Atmospheric and Planetary sciences

In collaboration with
Shell International Exploration and Production, Houston, Texas,
Geotomo LLC, Houston, Texas
and Prof. Dale Morgan

MIT Earth Resources Laboratory
2016 Annual Founding Members Meeting
May 18, 2016

Earth
Resources
Laboratory

Massachusetts
Institute of
Technology

Outline

Near-surface

- Few hundreds of meters below the surface ($\approx$ 500 m).
- Direct: Near-surface resources
  - Groundwater; Civil engineering; mineral resources
- Indirect: Near-surface imaging required for deep prospect resources
  - Statics correction
  - Oil exploration
- Near-surface challenges
  - rugged topography; large velocity variations; hidden layers

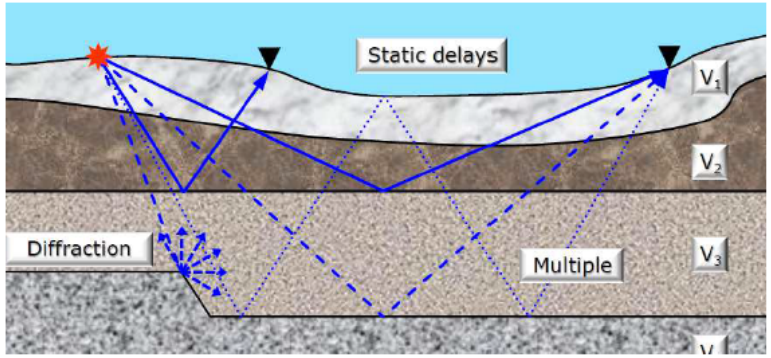

- Near-surface schematics
- Statics correction useful for focusing seismic reflection energy

Stack: Seismic only

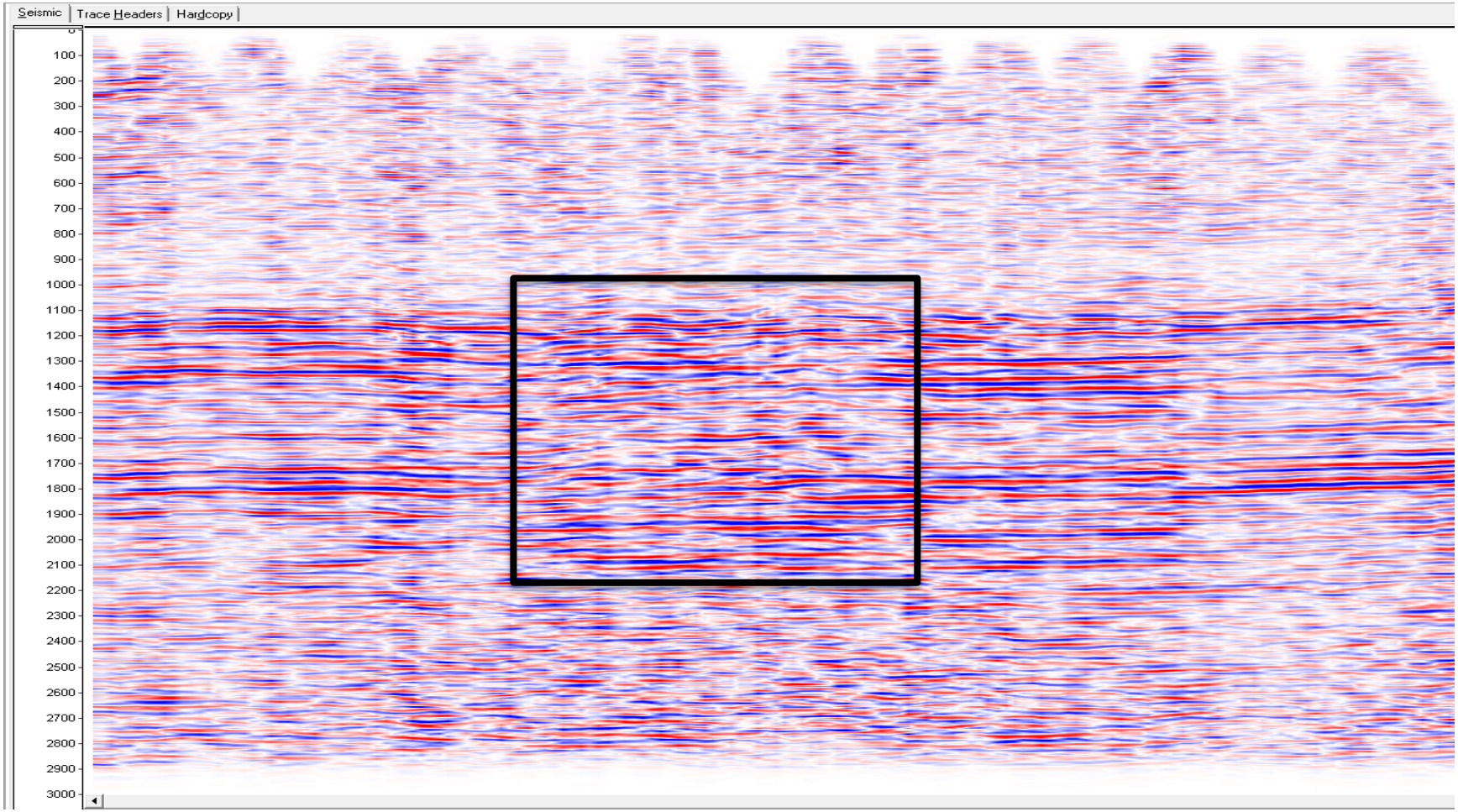

Stack: Joint inversion

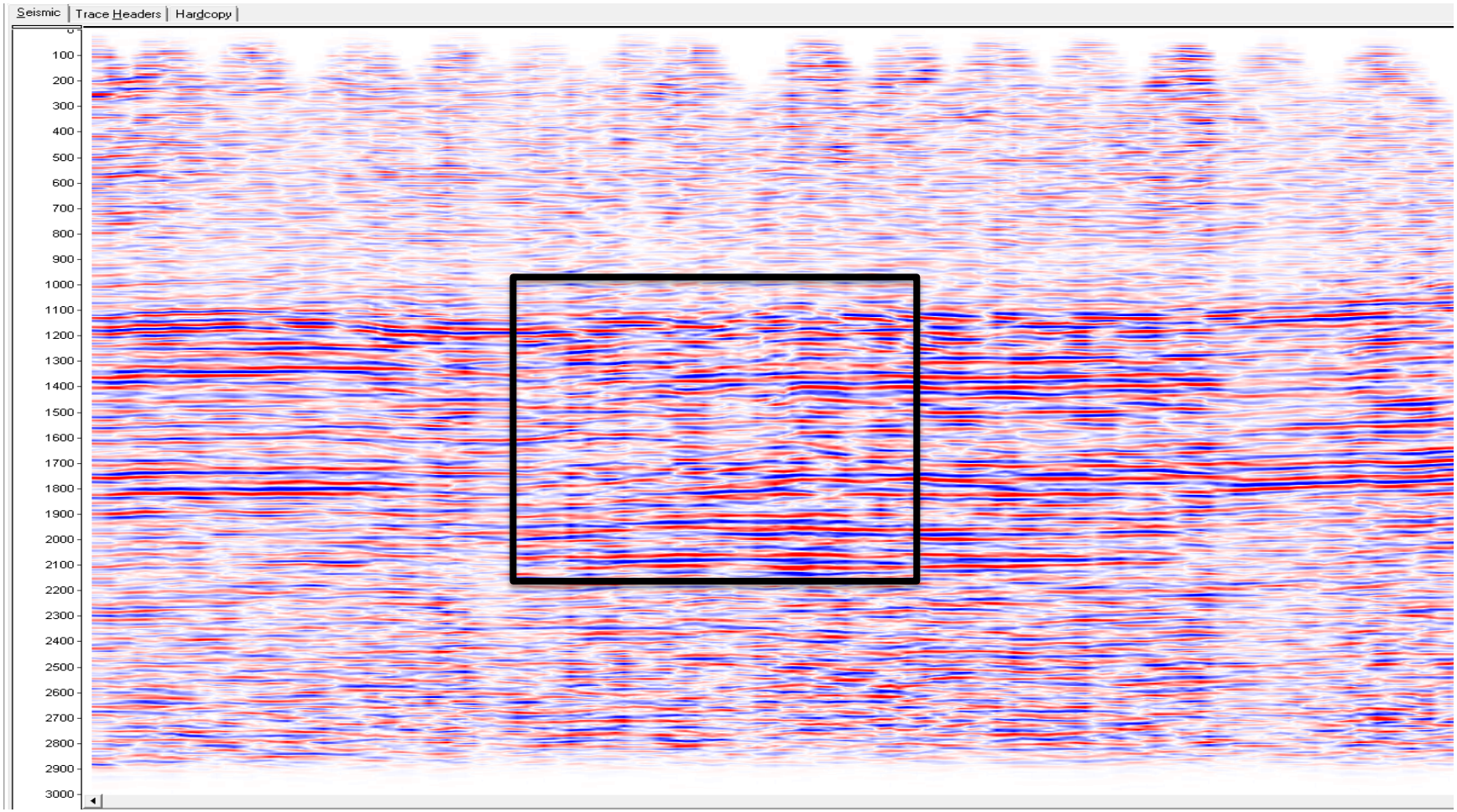

Joint inversion philosophy

- Subsurface geology: rock grain properties: physical, chemical, biological, etc. Their structures differ in dimensions: 1D, 2D or 3D.
- The more we know about a grain of rock the better for us identifying it uniquely.
- Unfortunately, geophysics only focuses on physical properties; and many of geophysical surveys just interpret a single physical property.

Joint inversion philosophy

- Therefore joint inversion philosophy suggests the use of multiple complementary geophysical data to improve on the unique identification of the subsurface.

- In my presentation today, although still few, I will show how two different types of data set (seismic traveltime and frequency EM data) can be used to improve the near-surface interpretation.

Objective

- Our objective in this study is to jointly invert 2D seismic data with 1-D airborne data but to resolve a 2D seismic velocity structure along with a 2D resistivity structure
- Both seismic velocity and resistivity models should be consistent in geological structures but different property values
- This effort will maximize the interpretation values of 2D seismic and 1-D airborne EM surveys.

Objective

- Therefore, our joint inversion problem is different from previous such efforts in which multiple datasets are acquired in the same 2D or 3D dimension
- We shall demonstrate the approach by using a 2D seismic dataset along with a Pseudo-2D frequency airborne EM dataset (from multiple 1D data set). The same method can be easily extended to 3D.

Collocated velocity and resistivity models

- Frequency airborne EM (FAEM) has similar principles with the TEM
  - However data are acquired in air (regardless of terrain)
  - Secondary vertical magnetic field measured in the presence of primary of magnetic field (limited resolution)
  - FAEM data in-phase or real component and quadrature or imaginary component of complex vertical magnetic field
- Seismic refraction tomography method:
  - Seismic refraction tomography data: traveltime recorded by the geophones

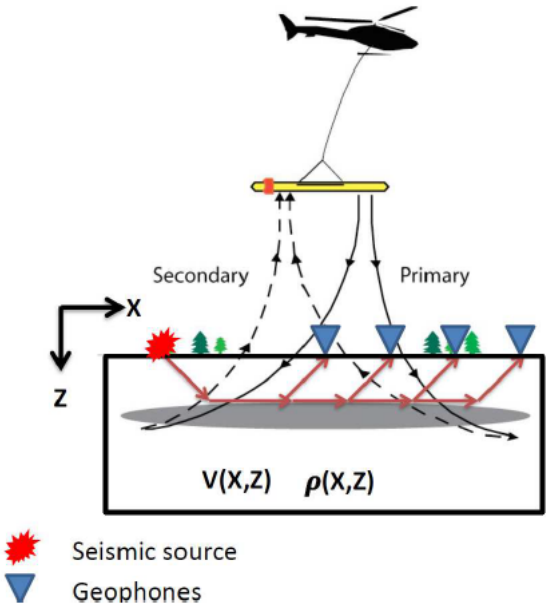

- Schematic diagram of FAEM system and seismic refraction experiment

Objective function

$$\phi(m_e, m_s) = \xi_e(\|\mathbf{W}_e(d_e - G_e(m_e))\|^2 + \tau_e\|\mathbf{L}m_e\|^2) + \xi_s(\|\mathbf{W}_s(d_s - G_s(m_s))\|^2 + \tau_s\|\mathbf{L}m_s\|^2) + \lambda\|t\|^2, \quad (1)$$

ξ_e, ξ_s: EM and seismic data misfit scaling factor: $\xi_e = 1 - \xi_s$,
L: regularization operator (derivative operator),
τ_e, τ_s: resistivity and velocity smoothing trade-off parameters,
W_e, W_s: EM and seismic traveltime data weights,
t, λ: cross-gradient and its weight,
m_s: 2D slowness model,
$G_s(m_s)$: calculated traveltime data on m_s,
m_e pseudo-2D resistivity model,
$G_e(m_e)$: calculated pseudo-2D EM data on m_e:

Cross-gradient constraints

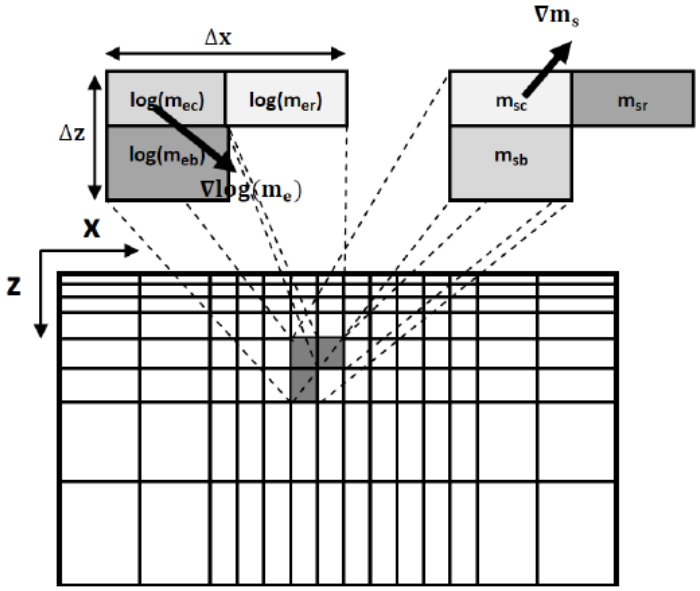

$$t(\log(m_e), m_s) = \nabla \log(m_e(x, y, z)) \times \nabla m_s(x, y, z) \qquad (2)$$

$$t(x, z) = \left(\frac{\partial \log(m_e(x, z))}{\partial z}\right)\left(\frac{\partial (m_s(x, z))}{\partial x}\right) - \left(\frac{\partial \log(m_e(x, z))}{\partial x}\right)\left(\frac{\partial (m_s(x, z))}{\partial z}\right) \qquad (3)$$

Iterative equation: conjugate gradient inversion method

$$\begin{pmatrix} \xi_e\left((\mathbf{W_e}\,\mathbf{A_e})^T\mathbf{W_e}\,\mathbf{A_e}+\tau_e\mathbf{L}^T\mathbf{L}\right)+\lambda\mathbf{B_e}^T\mathbf{B_e} & \mathbf{0} \\ \mathbf{0} & \xi_s\left((\mathbf{W_s}\,\mathbf{A_s})^T\mathbf{W_s}\,\mathbf{A_s}+\boldsymbol{\tau_s}\mathbf{L}^T\mathbf{L}\right)+\lambda\mathbf{B_s}^T\mathbf{B_s} \end{pmatrix}\begin{pmatrix} \Delta m_e^{k+1} \\ \Delta m_s^{k+1} \end{pmatrix}$$

$$= \begin{pmatrix} \beta\left(\xi_e\left((\mathbf{W_e}\,\mathbf{A_e})^T\mathbf{W_e}\Delta d_e-\tau_e\mathbf{L}^T\mathbf{L}m_e^k\right) & -\lambda\mathbf{B_e}^T t\right) \\ \xi_s\left((\mathbf{W_s}\,\mathbf{A_s})^T\mathbf{W_s}\Delta d_s-\tau_s\mathbf{L}^T\mathbf{L}m_s^k\right) & -\lambda\mathbf{B_s}^T t \end{pmatrix}$$

$$\begin{pmatrix} m_e^{k+1} \\ m_s^{k+1} \end{pmatrix} = \begin{pmatrix} m_e^k \exp\left(\Delta m_e^{k+1}\right) \\ m_s^k+\Delta m_s^{k+1} \end{pmatrix}, \quad k = 1,2,3,\ldots,N.$$

The model update $\begin{pmatrix} \Delta m_e^{k+1} \\ \Delta m_s^{k+1} \end{pmatrix}$ is found by the conjugate gradient (CG) method.

$\mathbf{B_e}$ and $\mathbf{B_s}$ are resistivity and slowness model cross-gradient sensitivity matrices respectively.

The cross-gradient sensitivity is the partial derivative of t with respect to the model parameters.

β is the model weighting

Synthetic data example

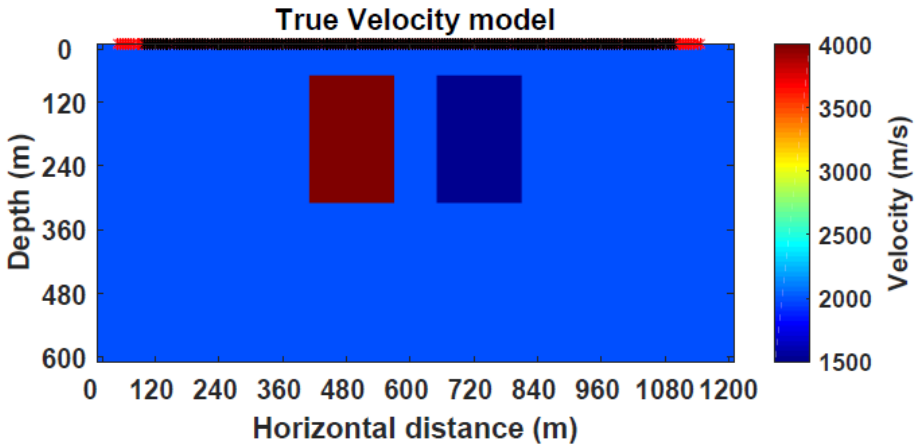

- High/Low velocity: 4000m/s; 1500m/s; 60m deep
- Seismic geometry: 360 shots; 200 receivers
- Shot-receiver offset range 0.5 to 1042.5m

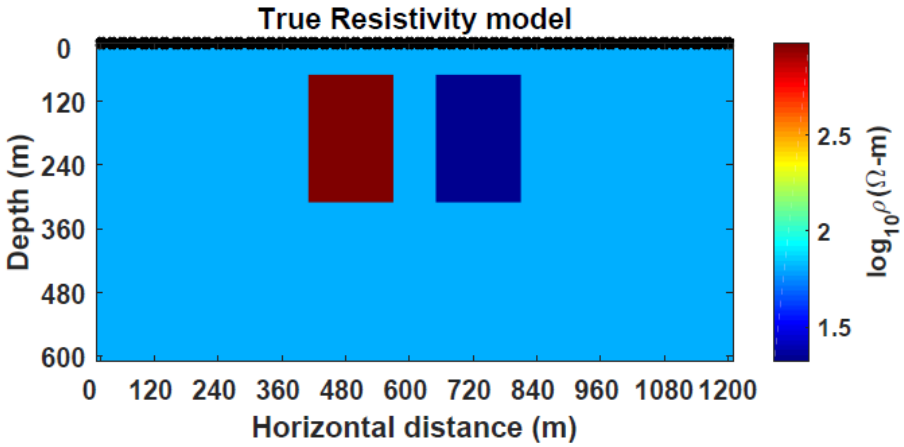

- High/Low velocity: 946 Ohm-m; 21 Ohm-m; 60m deep
- EM geometry: 60 locations ; 20m separation; 50m altitude; 7.93 coil separation
- Frequency range 0.1Hz to 100kHz

Raycounts and sensitivity analysis

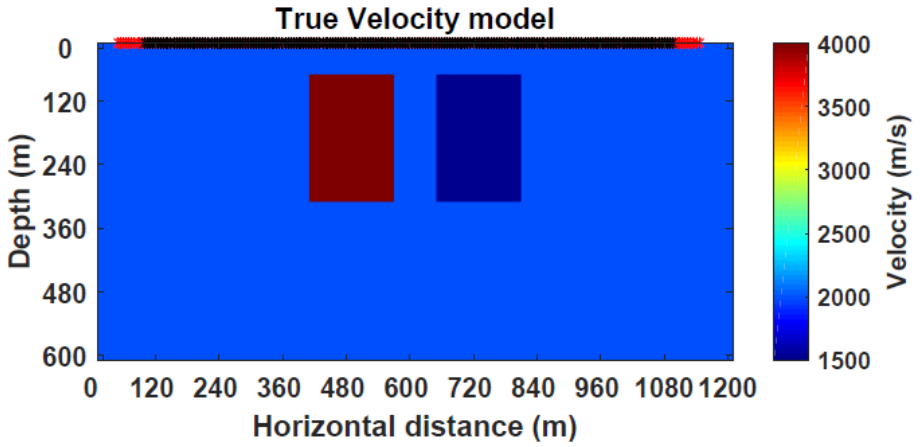

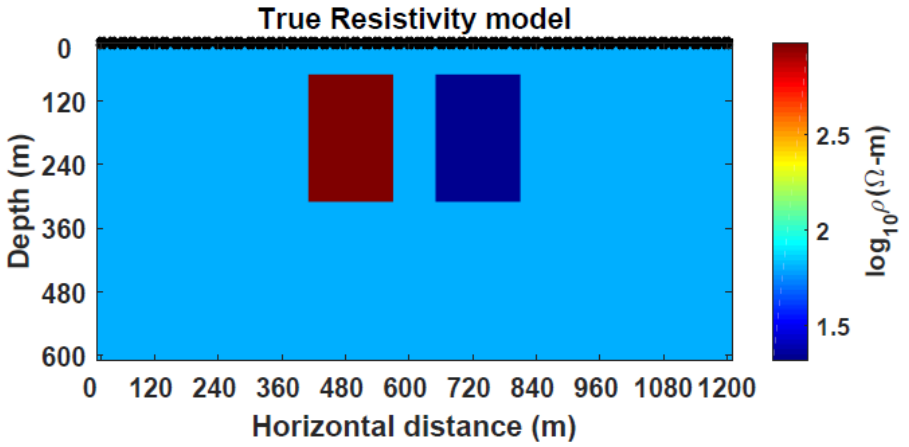

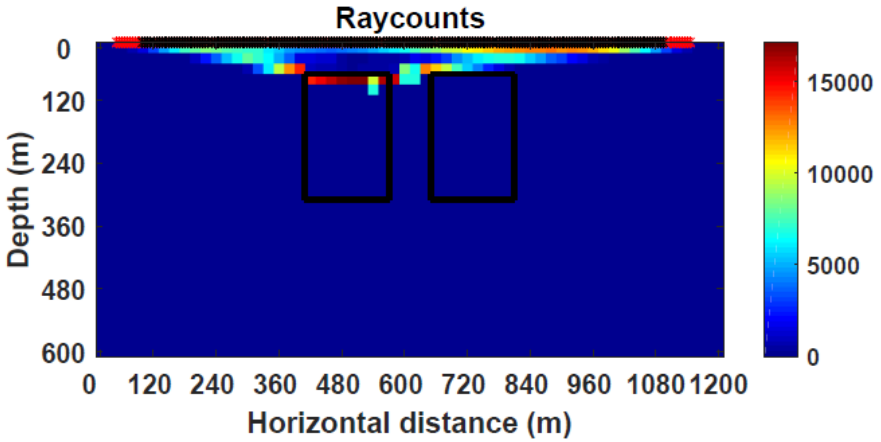

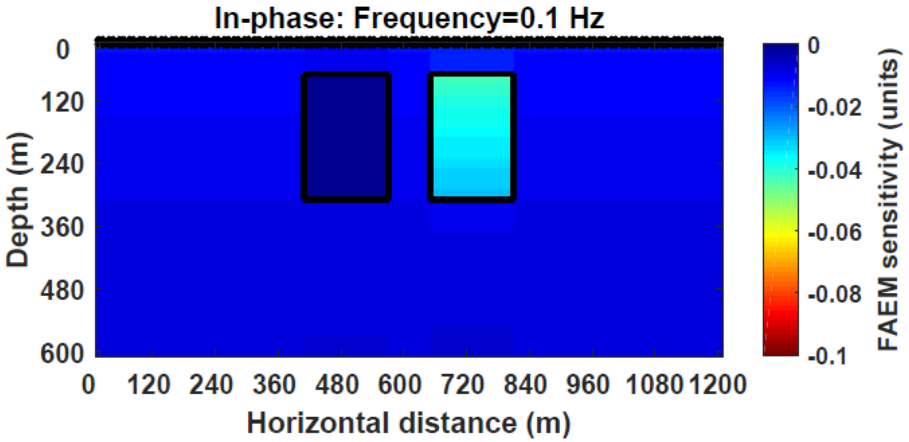

Anticipation from raycount and sensitivity analysis

- Refraction seismology cannot image bottom of block:
  - when moving from high to low velocity medium
- Frequency domain EM, inductive method, is more sensitive to the conductive block than the resistive one, yet still provides a wide spectrum
  - that helps to image the different parts of the blocks
- We therefore anticipate the EM method will image the resistivity structure
- And communicate that to velocity model during the joint inversion

Standalone inversion

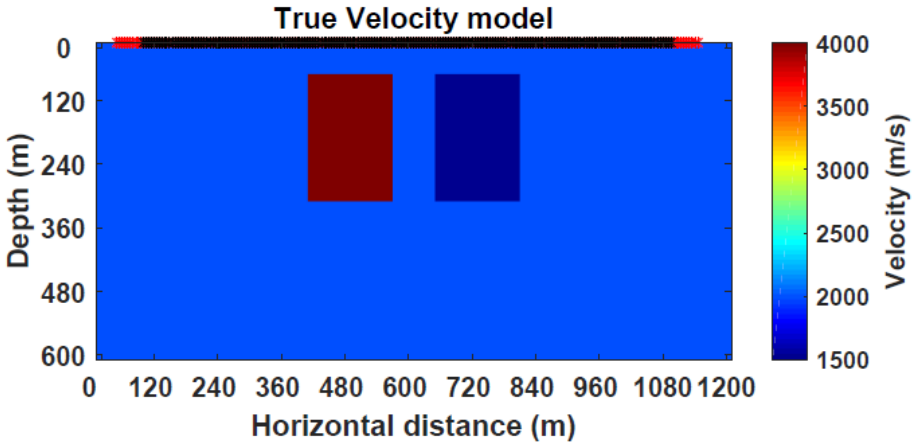

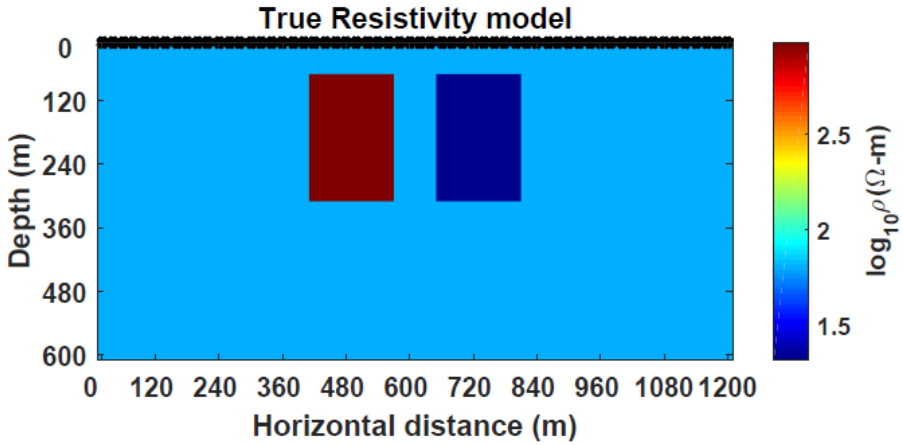

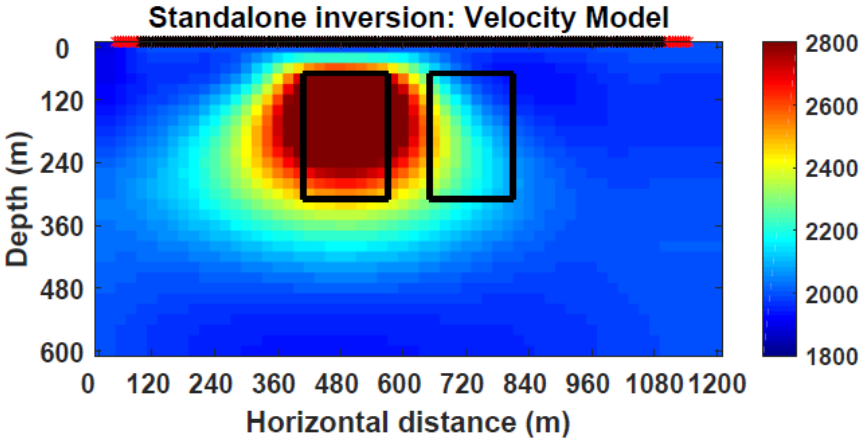

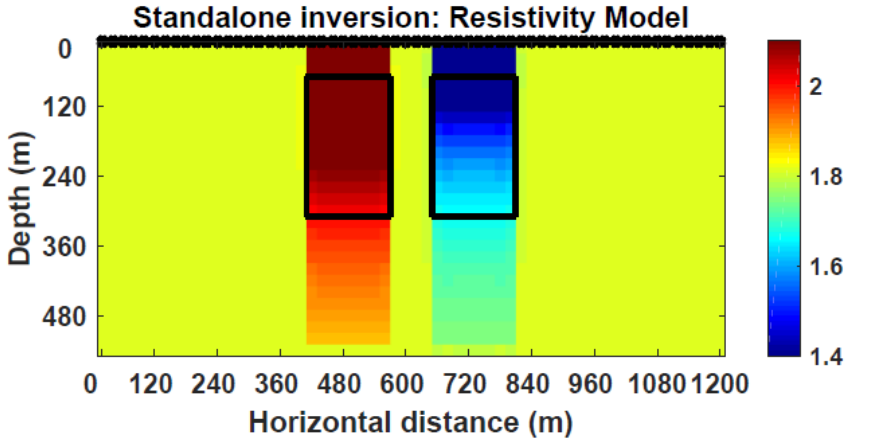

Joint inversion parameter settings

- From the objective function different weights have to be supplied and balanced for optimum results
  - Data weight W_e, W_s,set as unity (Synthetic)
  - Data misfit weights $\xi_e = 0.7$; $\xi_s = 0.3$
  - Model weight, $\beta = log(max(m_e)) * min(m_s)$; $\beta = 0.0017$.
- Cross-gradient weight, λ
  - We will appreciate the selection of λ by performing the joint inversion for 2 different initial models
  - **A: Initial model: 4 iterations (standalone) are done**
  - **B: Initial model: Homogeneous**
  - $\lambda = 0.1, 0.3, 1, 3, 300, 10000$

Joint inversion parameter settings

Initial Model

Initial model: after four iterations for separate inversion

Joint inversion results: Cross-gradient weights

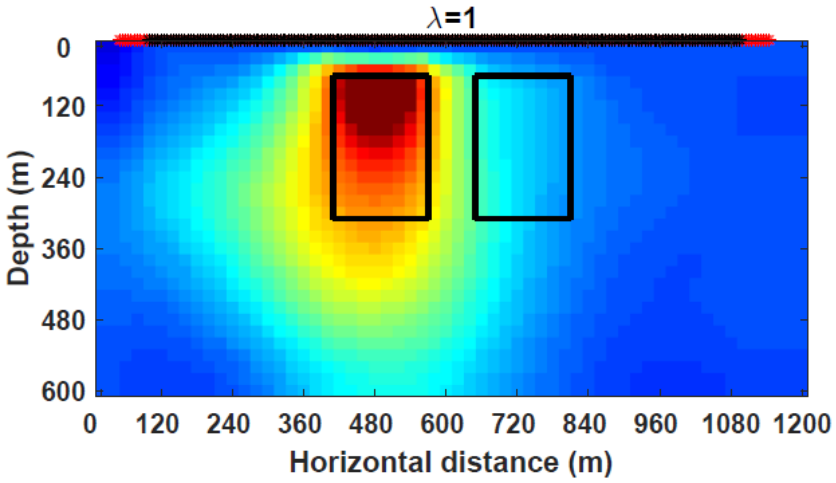

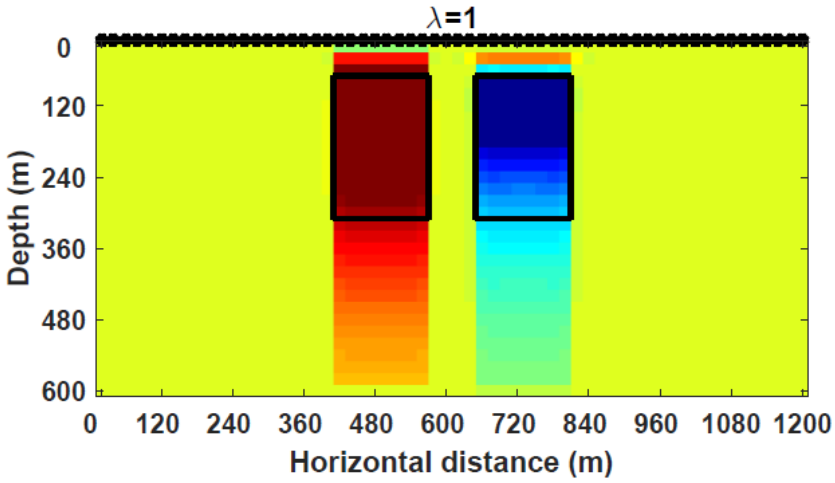

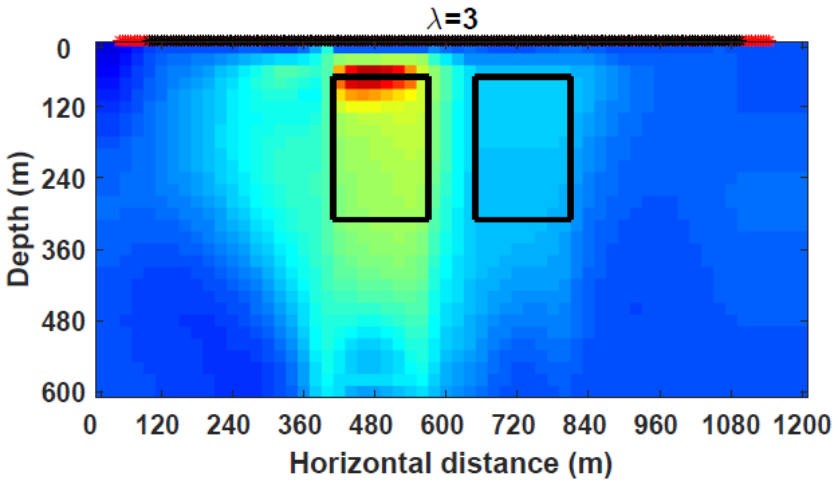

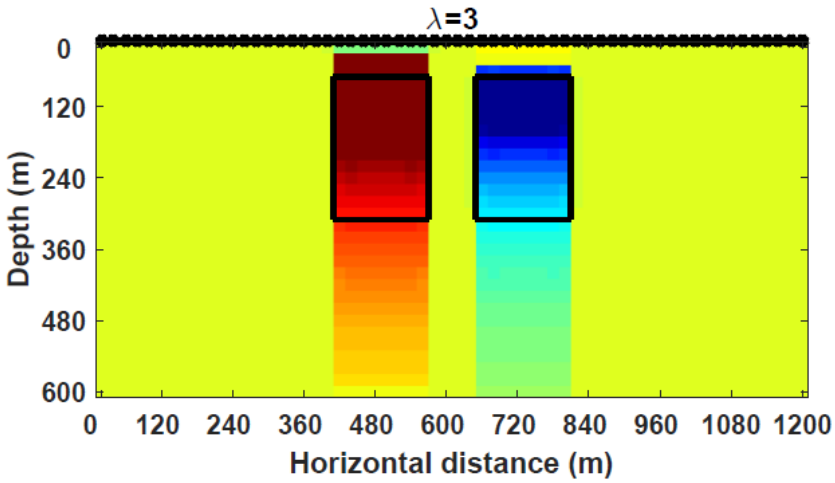

Joint inversion parameter settings

Initial Model

Homogeneous initial model

Joint inversion results: Cross-gradient weights

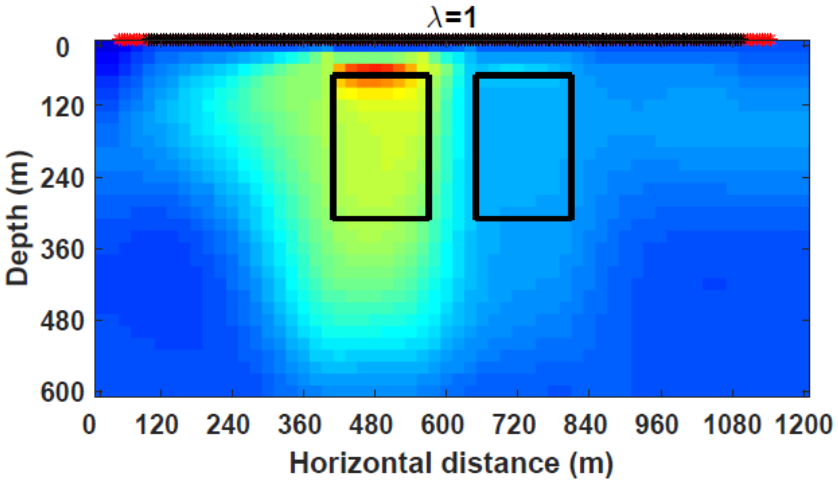

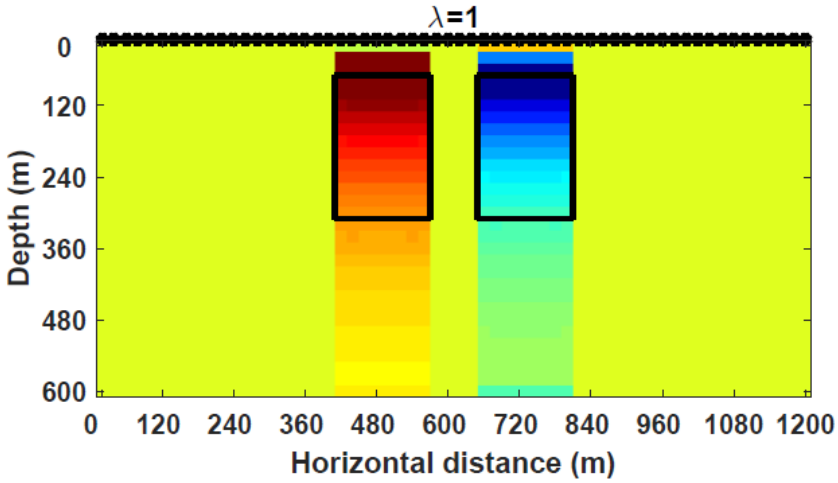

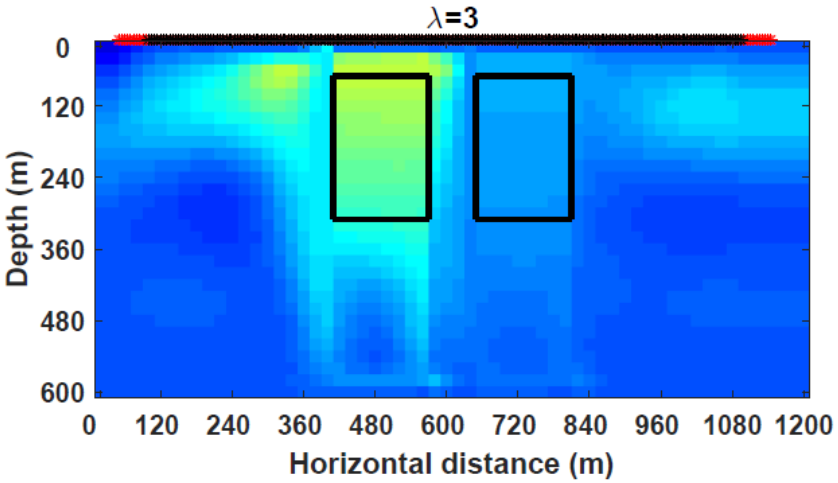

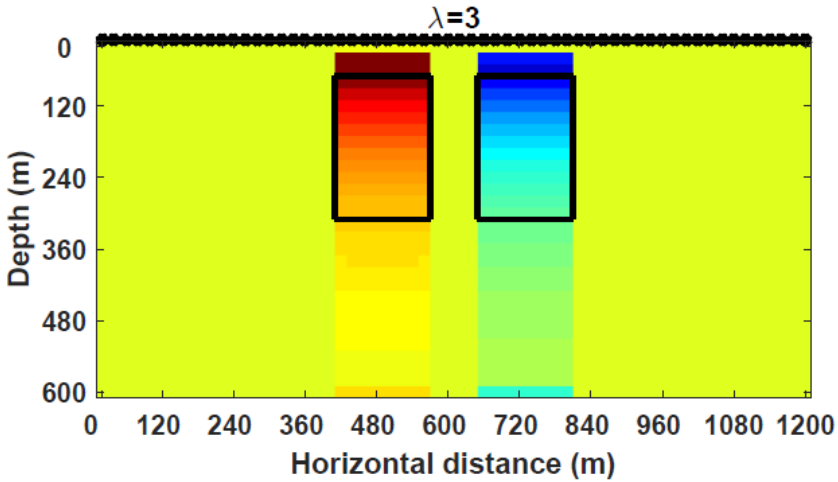

Compare Initial models: homogeneous (up); 4 iterations (down)

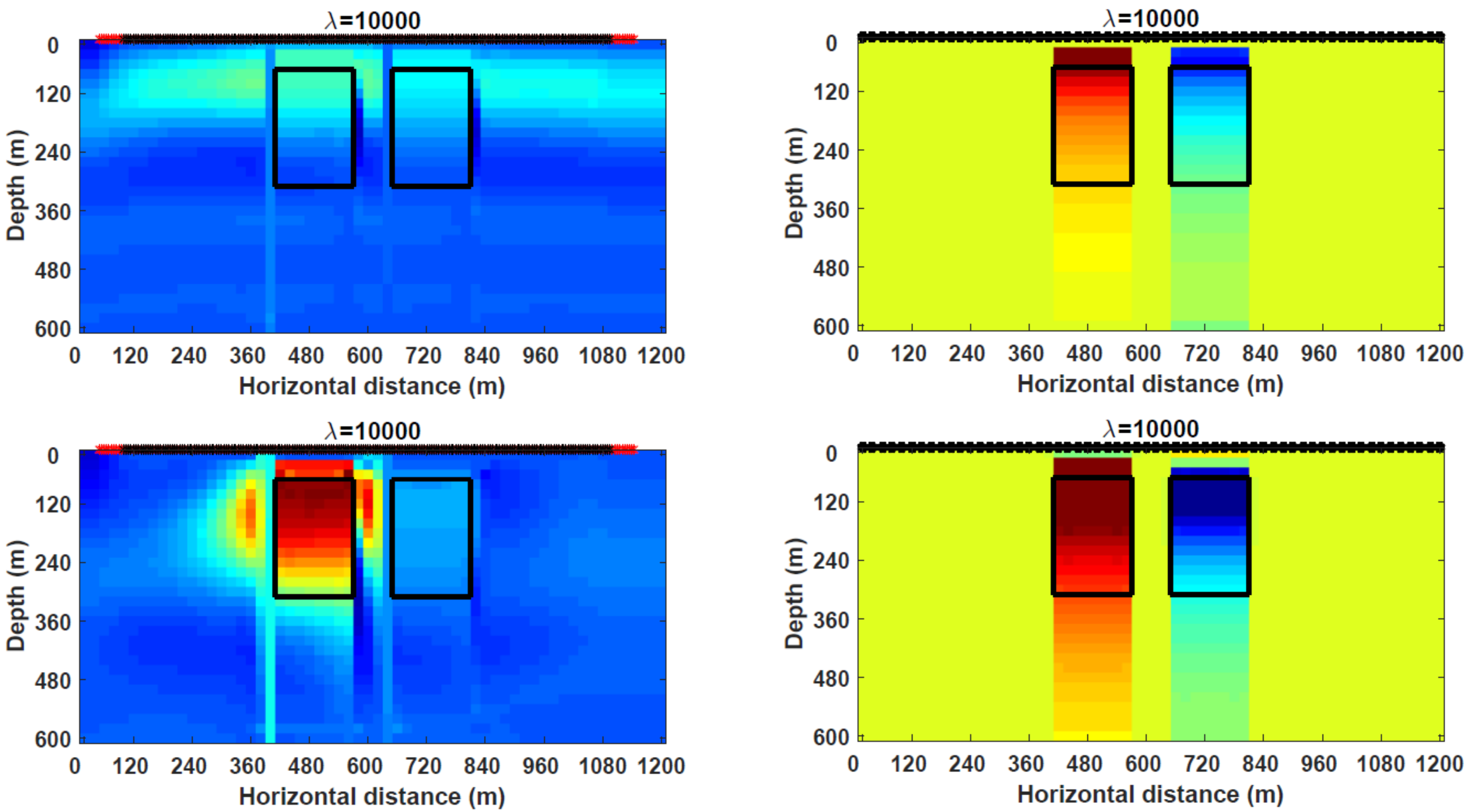

MISFIT PLOTS: Cross-gradient after 4 iterations

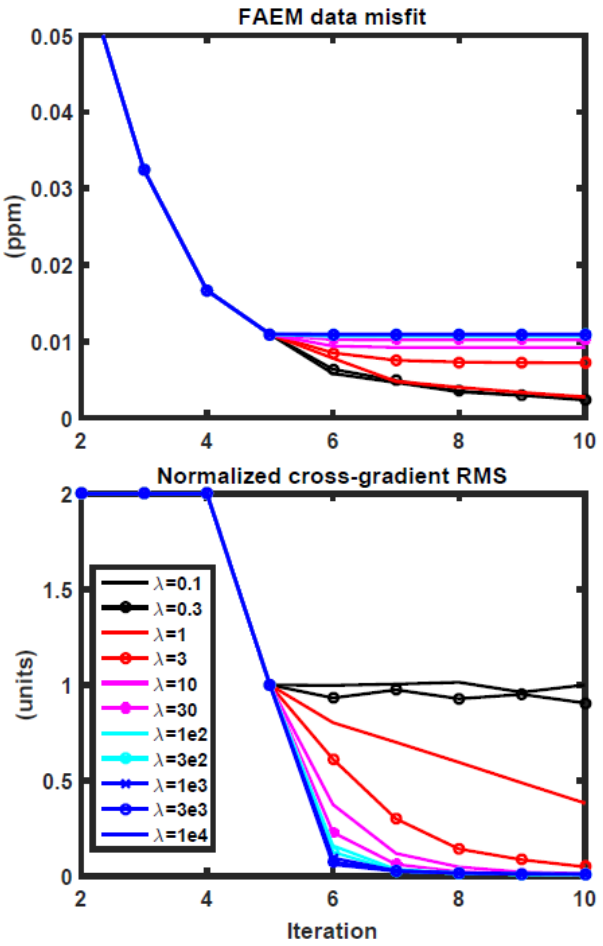

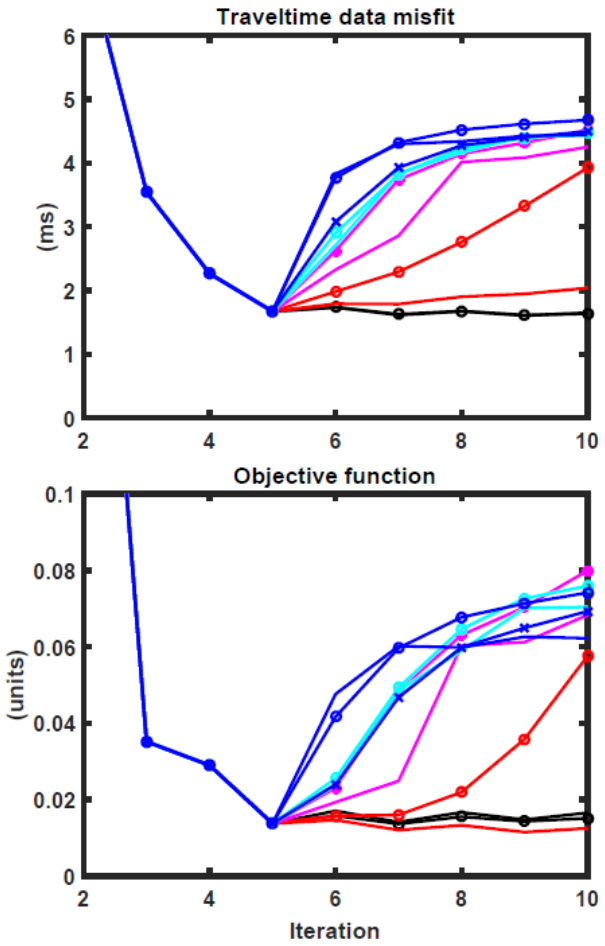

MISFIT PLOTS: Homogeneous initial model

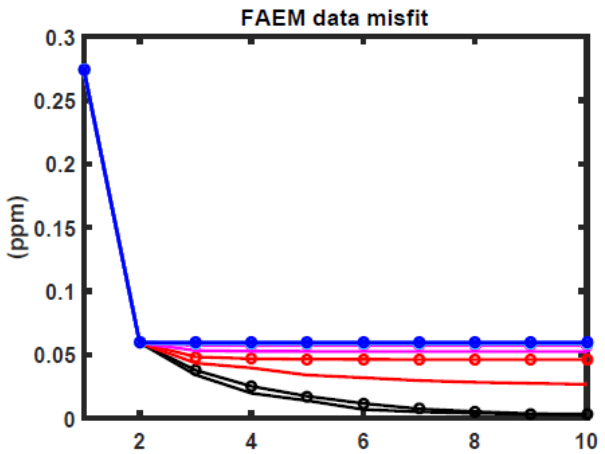

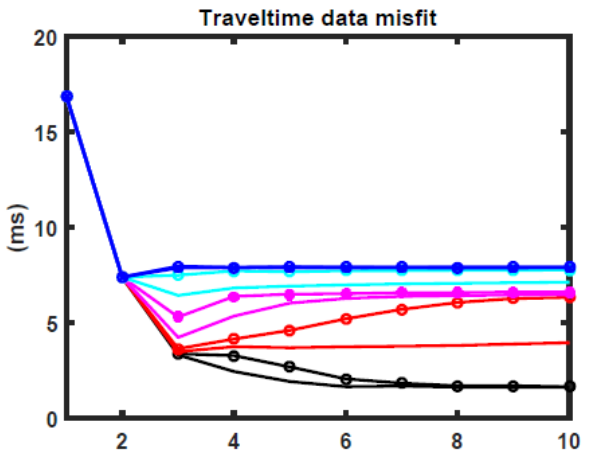

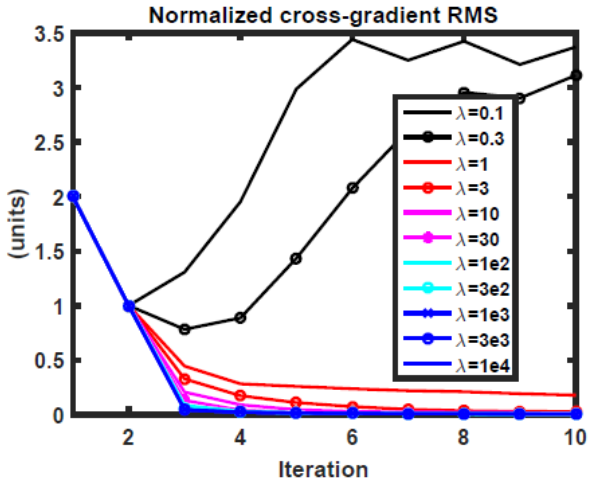

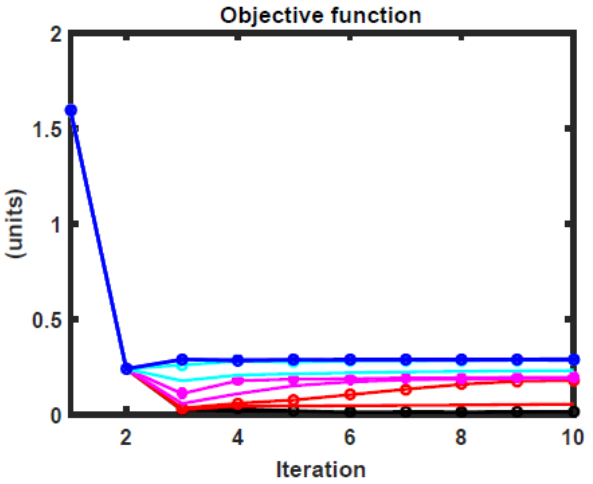

Field data example

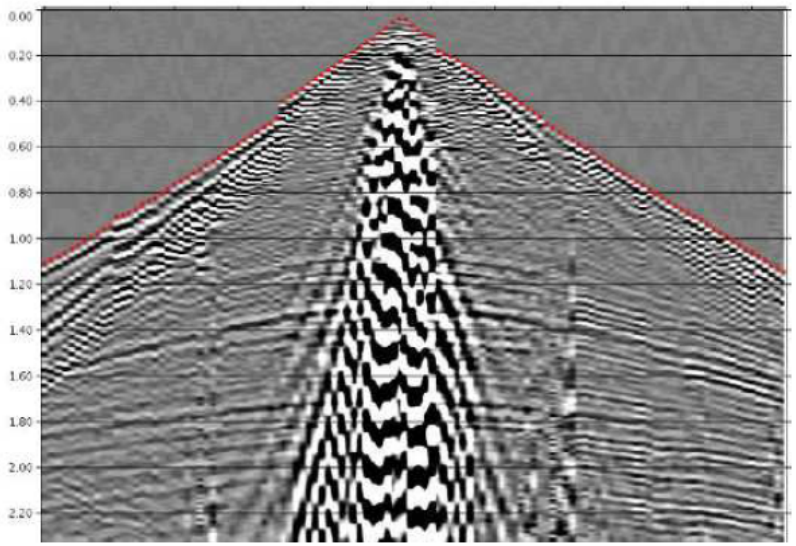

- Collocated velocity and resistivity models: 10 km
- Seismic geometry: 191 shots; 82 receivers; 50 m shot spacings
- First break picked on common receiver gather: sparsity of data

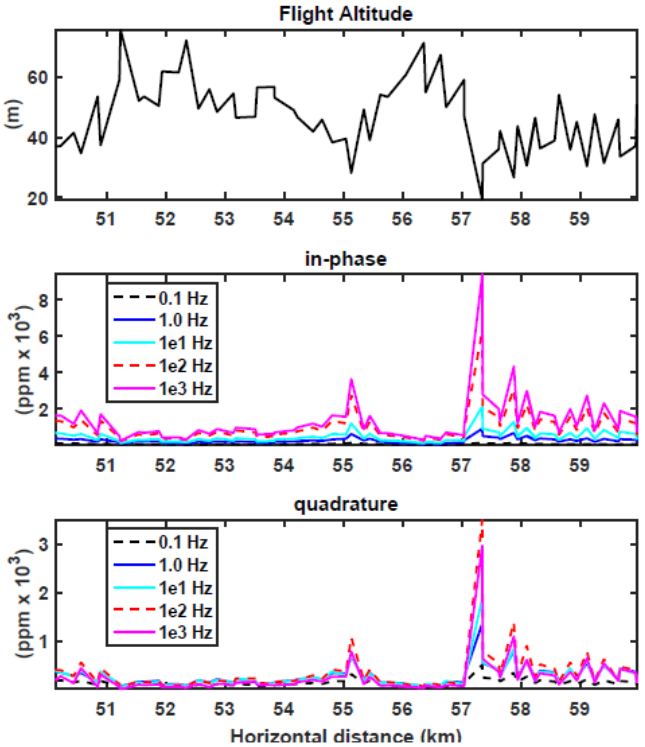

- CGG Airborne RESOLVE; 62 FAEM data points
- Frequencies: 390; 1,787; 8391; 40,740; 131,630 Hz

Joint inversion parameter settings

- Different weights used
  - Data weight W_e, W_s
  - Model weight, $\beta = 0.001$
  - Cross-gradient weight $\lambda = 10$
- Initial velocity model is built from traveltime picks
- Standalone velocity model inversion is performed
- This velocity is empirically converted to resistivity model
- Standalone resistivity model inversion is done
- The joint inversion workflow begins: standalone models

Standalone inversion: models

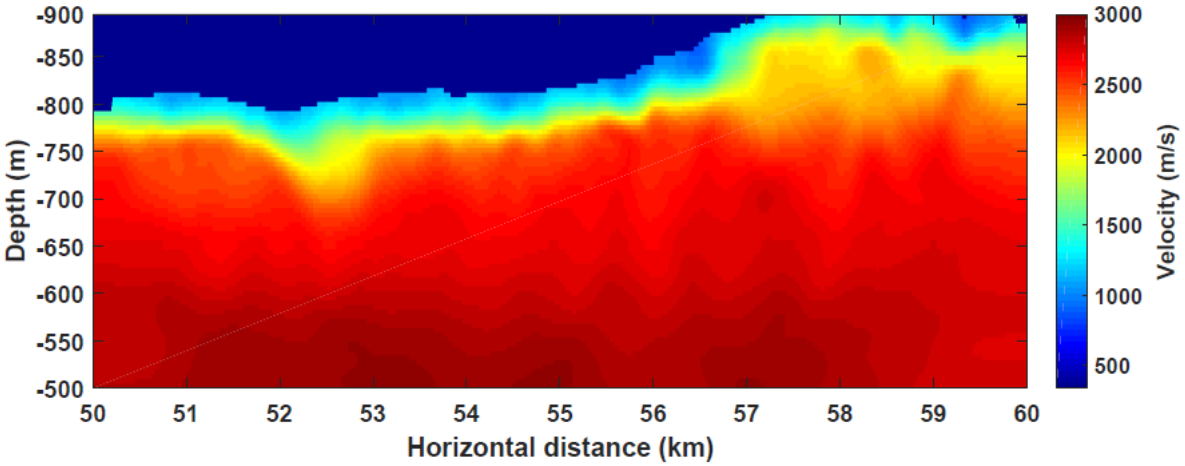

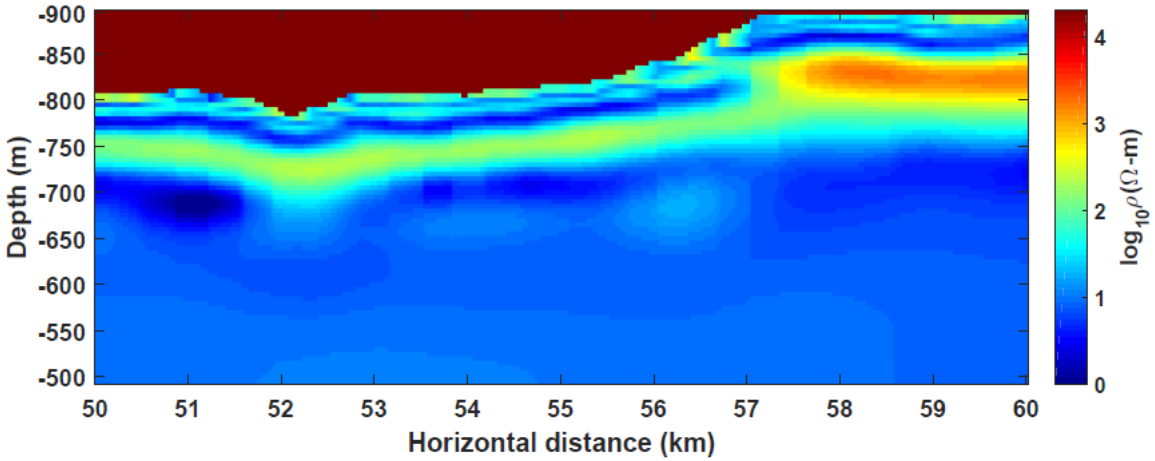

- Velocity model
- Statics corrections (Long-wavelength)
  - Weathering velocity
  - Sub-weathering (replacement) velocity
- Resistivity model

Joint inversion: models

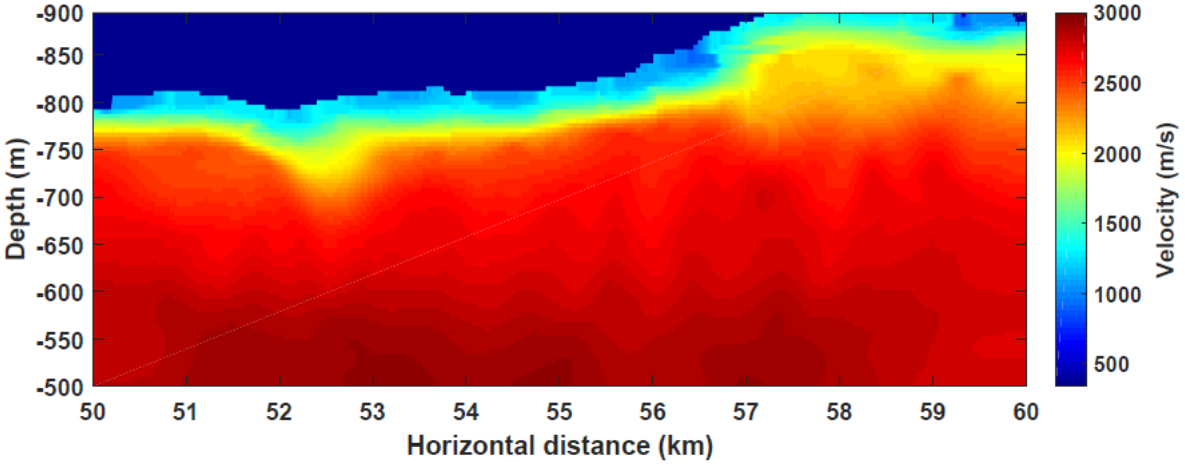

- Velocity model
- Statics corrections (Long-wavelength)

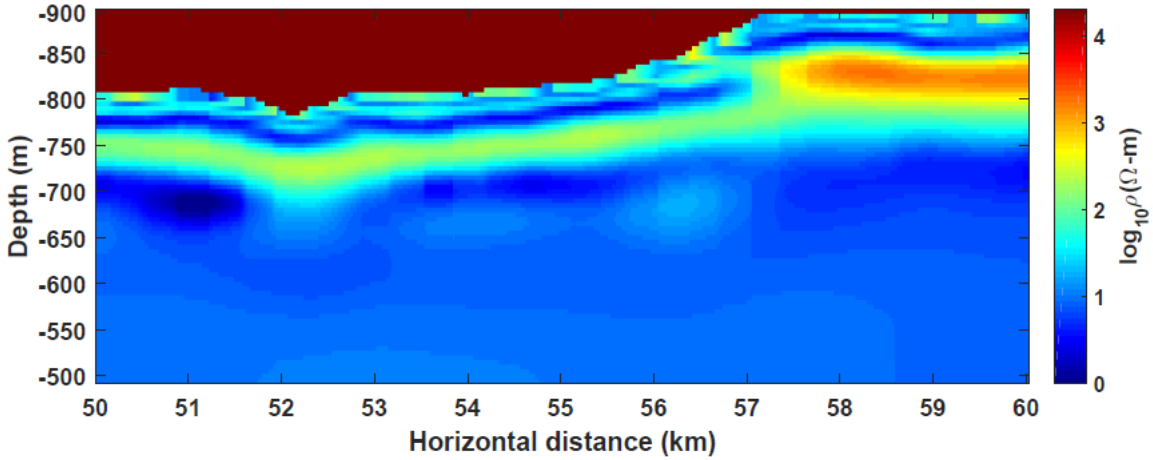

- Weathering velocity
- Sub-weathering (replacement) velocity

- Resistivity model

Stack imaging workflow

- Geometry correction to map 3D geometry along a 2D line traverse.
- Spherical divergence correction.
- Decovolution with a prediction leg of 20 ms.
- Spectral whitening.
- Statics correction
  - Velocity from standalone traveltime tomography
  - Velocity from joint inversion
- Dipping filter to remove coherent noise.
- NMO correction
- CMP stack and amplitude gain control

Stack: Seismic traveltime statics

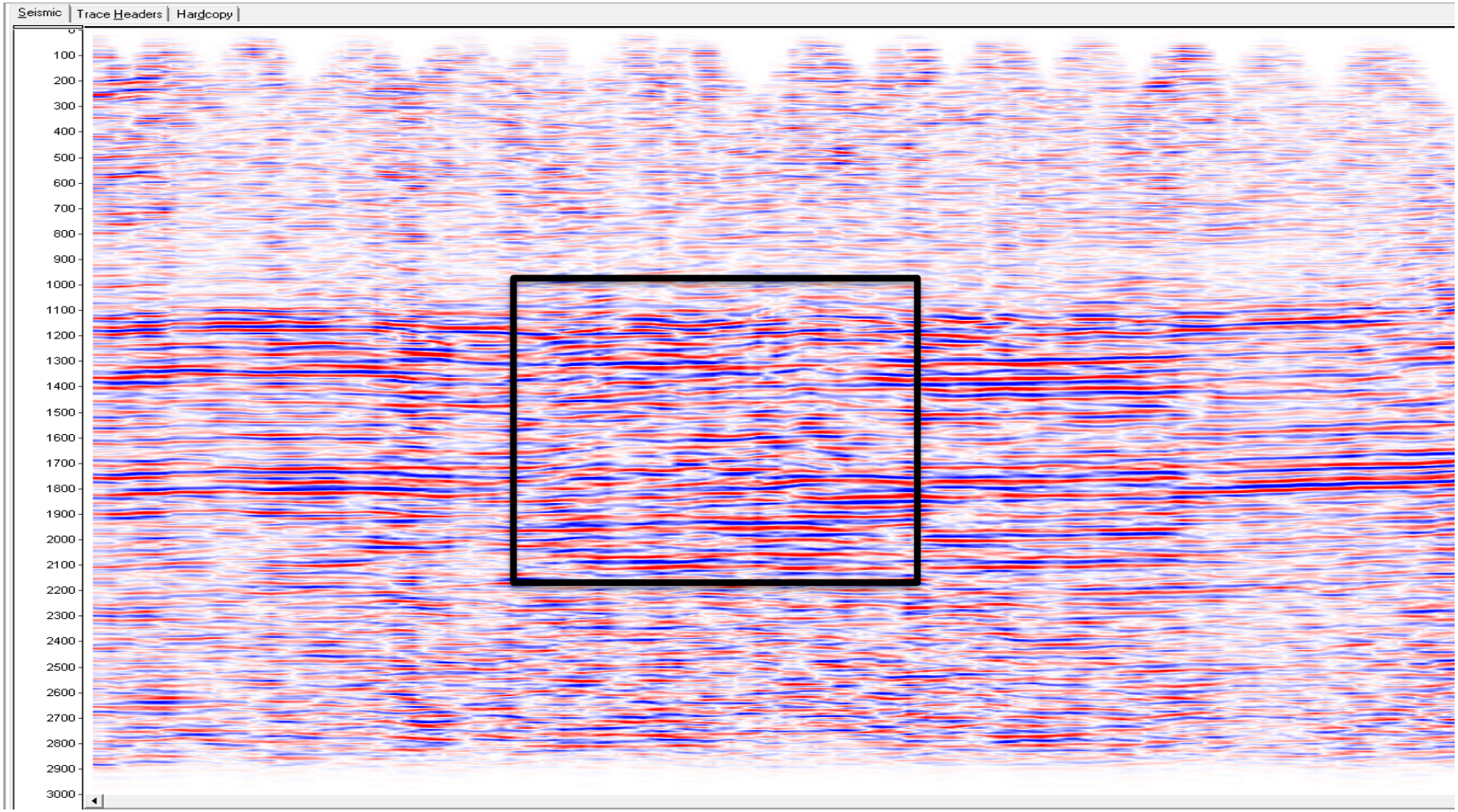

Stack: joint inversion statics

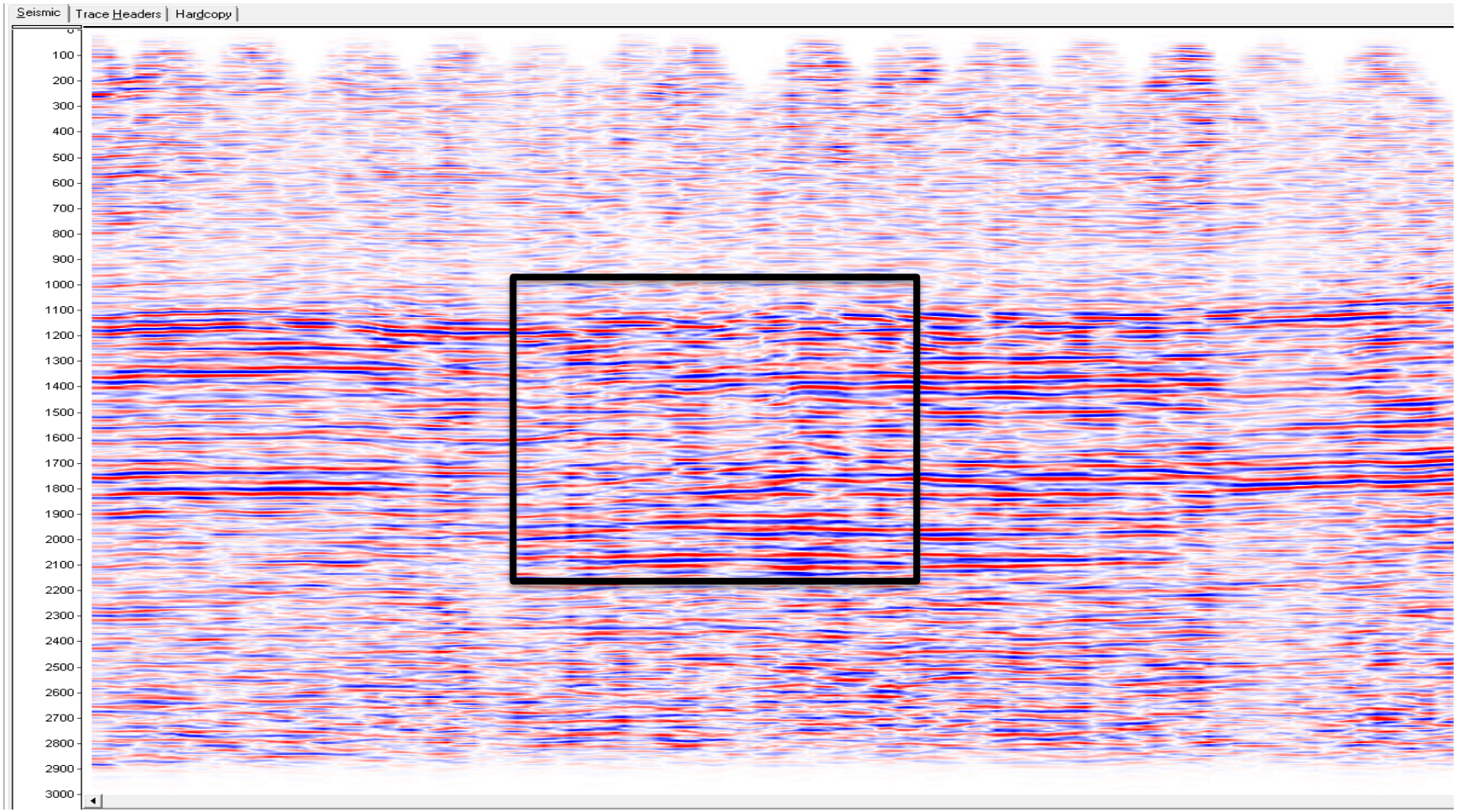

Conclusions

- Perform joint inversion on different spatial geometries of velocity and resistivity model
  - Traveltime data from 2D geometry and frequency airborne EM data from multiple 1D from which pseudo-2D geometry is formed.
  - Parameter settings are discussed
  - Performance depends on good initial velocity and resistivity models
  - Remarkable improvement of the near-surface by joint inversion compared to standalone results.

Thank you!

Conclusions

Fitterman, D.V., and W.L. Anderson, 1987, Effect of transmitterturn-off time on transient soundings: Geoexploration, 24, 131-146.

Ingeman-Nielsen, T., and F. Baumgartner, 2006, CR1Dmod: a matlab program to model 1D complex resistivity effects in electrical and electromagnetic surveys: Computers and Geosciences, 32, 1411-1419.

Meju, M.A., 1994, Geophysical data analysis: understanding inverse problem theory and practice. Society of Exploration Geophysicists course notes series, No. 6, 1st edition: SEG.

Muja, M., and D.G. Lowe, 2009, Fast approximate nearest neighbors with automatic algorithm configuration: VISAPP, 1, 331-340.

Nekut, A.G., 1987, Short note: direct inversion of time-domain electromagnetic data: Geophysics, 52, 1431-1435.

Wang, H.P., 2004, Digital filter algorithm of the sine and cosine transform: Chinese Journal of Engineering Geophysics, 1, 329-335.

Ward, S.H., and G.W. Hohmann, 1987, Electromagnetic theory for geophysical applications, in M.N. Nabighian, ed., Electromagnetic methods in applied geophysics v.1: SEG, 131-311.

Zhang, J., and F, D., Morgan, 1996, Joint seismic and electrical tomography. Paper presented at EEGS Symposium on Applications of Geophysics to Engineering and Environmental Problems, Environ. and Eng. Geophysics Society Keystone Colo.

Zhang, J., and M, N., Toksöz, 1998, Nonlinear refraction traveltime tomography: Geophysics, 63, 1726-1737.

Zhang, J., H. Zhang, E. Chen, Y. Zheng, W. Kuang and X. Zhang, 2014, Real-time earthquake monitoring using a search engine method: Nature communications, doi: 10.1038/ncomms6664.